PCCP

PAPER

View Article Online
View Journal | View Issue

Cite this: *Phys. Chem. Chem. Phys.*, 2016, **18**, 13459

Gold nanoparticles in aqueous solutions: influence of size and pH on hydrogen dissociative adsorption and Au(III) ion reduction†

B. G. Ershov,* E. V. Abkhalimov,* R. D. Solovov and V. I. Roldughin

Received 25th March 2016,
Accepted 20th April 2016

DOI: 10.1039/c6cp01996j

www.rsc.org/pccp

The shift of the localized surface plasmon resonance (LSPR) band of gold nanoparticles to shorter wavelengths upon saturation of the hydrosol with hydrogen is used as a tool to study the electrochemical processes on the particle surface. It is shown that dissociative adsorption of hydrogen takes place on the surface of a particle and results in the migration of a proton into the dispersion medium, while the electron remains on the nanoparticle, *i.e.*, a hydrogen-like nanoelectrode is formed. It is shown that Au(III) ions can be reduced on the gold nanoelectrodes. A thermodynamic scheme explaining the shift of the LSPR band is used to explain the peculiarities of the Au(III) ion reduction. The reduction rate does not depend on the ion concentration and varies linearly with pH. The observed correlations are explained in terms of a simple model of electrochemical processes taking place on the nanoparticle as an electrode. It is shown that with an increase in the particle size, its capacity for dissociative adsorption of hydrogen decreases and the Au(III) reduction slows down.

Introduction

Bulk gold is a chemically inert metal exhibiting no catalytic activity, while nanosized gold (up to 5 nm) deposited on various substrates catalyzes a variety of reactions of organic synthesis.[1–4]

The gold hydrosol shows intensive absorption in the visible region caused by collective excitation of the conduction electrons by light. The optical properties of the hydrosol depend substantially on the size of nanoparticles, density of electrons in them and properties of the dispersion medium and interface.[5] It is clear that the change in the electron density (concentration) in the particles results in a shift of the localized surface plasmon resonance (LSPR) band.[6–10] The electron density can be changed in many ways, for example, by adsorption of electron acceptors or donors on the nanoparticle surface. Thus, the shift of the plasmon resonance could serve as a tool for the study of the processes taking place at the surface of the nanoparticles. In particular, it was used to study the adsorption of gases on gold nanoparticles in aqueous medium.[11–15] It has been shown that saturation of the hydrosol with ozone induces a reversible shift of the LSPR band to longer wavelength. This shift of the band manifests a size effect: the smaller the nanoparticle size, the greater the shift. The shift of the band was explained by variations of the electron density.[13] That is, the smaller the gold particles, the greater the decrease in the electron density of nanoparticles as a result of shifting of conduction electrons to adsorbed ozone molecules. Conversely, the adsorption of oxygen or nitrous oxide does not induce noticeable change in the LSPR band that indicates their weak bonding with the surface of nanoparticles.[13]

Hydrogen adsorption and dissociation are elementary steps in many reactions involving hydrogen and catalyzed by noble metal (in particular, gold) nanoparticles. We considered it promising to study these phenomena by electron spectroscopy in the gold hydrosol. The mechanism of hydrogen adsorption on gold nanoparticles can be identified by the shift of the plasmon resonance. The influence of various factors (first of all, particle size and pH) on the process can also be revealed by the pattern of plasmon absorption variation. Previously,[16] it was shown that the saturation of a gold hydrosol (3 nm particles were used) with hydrogen induces a shift of the LSPR band to the shorter wavelengths. This indicates that the density (or concentration) of electrons in the nanoparticles increases. In other words, hydrogen molecules, unlike ozone, are electron donors. This suggests the dissociative adsorption of the hydrogen on the nanoparticle surface. The use of gold particles of different size and solutions with different pH (from 3.5 to 11.5) confirmed this assumption. A critical size (20–30 nm) above which gold particles are unable to adsorb hydrogen by the dissociative mechanism was established. It was also shown that overpotential on nanoparticles predetermines the possibility of

A. N. Frumkin Institute of Physical Chemistry and Electrochemistry, Russian Academy of Science, Leninsky pr. 31-4, Moscow, 119071, Russia. E-mail: ershov@ipc.rssi.ru, abkhalimov@ipc.rssi.ru

† Electronic supplementary information (ESI) available. See DOI: 10.1039/c6cp01996j

Au(III) reduction. The particle overpotential and the rate of the catalytic reduction of Au(III) ions with hydrogen were shown to depend linearly on the pH.

Experimental

Preparation of Au nanoparticles

The gold hydrosol was synthesized using tetrachloroauric(III) acid trihydrate, sodium borohydride, and sodium citrate, all ACS Reagent Grade chemicals (Aldrich). Solutions were prepared with distilled water, which was additionally deionized on an Arium 611 unit (Sartorius, Germany) and had a specific electrical conductivity of not more than 0.056 μS cm^{-1}.

Gold nanoparticles with average sizes of 4.6, 7.8, and 12.2 nm were prepared by pulsed photochemical reduction of Au(III) in aqueous solutions.[17] Particles of different sizes were obtained by varying the initial Au(III) concentration and pulsed radiation time. A previous study[18] has indicated that the particles with an average size of 4.6 nm prepared by this technique were not twinned but single domain crystals.

Gold particles with sizes of 19 and 28.2 nm were synthesized by the Turkevich procedure.[19,20] Gold hydrosols with a mean particle size of 4.6 and 28.2 nm were used as primary subjects of this study.

Saturation with hydrogen

The experiments on hydrogen adsorption on Au nanoparticles were performed as follows. An aliquot of a desired gold colloidal solution (4 mL) was placed into a special cell equipped with a quartz cuvette with a light path of 10.0 mm. The cell design allowed evacuation of it and isolation of its internal volume from the environment. Then hydrogen was injected into the cell. After the optical spectrum was measured, hydrogen was removed from the colloidal solution by vacuum pumping for 20–30 s. After this, the residual hydrogen concentration in the solution did not exceed 10^{-6} mol L^{-1}.

Catalysis

The catalysis was carried out as follows. For the catalytic reduction of Au(III), 1 mL gold hydrosol was mixed with a 2 mL of Au(III) aqueous solution, and a 1 mL trisodium citrate solution. The concentrations of the gold catalyst and trisodium citrate in all solutions were 0.05 mmol L^{-1} and 1 mmol L^{-1} respectively. The resulting solution was stirred using a magnetic stirrer for 1 h; then, it was deaerated and saturated with hydrogen.

For keeping a constant pH value in solutions, the Britton–Robinson buffer was used.[21]

Characterization

The absorption spectra of gold colloidal solutions were measured at specified time intervals (up to several days) using a Cary 100 Scan UV-Visible spectrophotometer (Varian Inc.) equipped with a thermostated cuvette compartment at 20 °C (wavelength range 190–900 nm, bandwidth 2 nm, integration time 0.1 s, data interval 1 nm, scan speed 600 nm min^{-1}).

The sizes and shapes of the gold nanoparticles were also analyzed using a Leo-912 AB Omega (Carl Zeiss) and JEM-2100 (JEOL) transmission electron microscope. For this purpose, a droplet of a colloidal solution was kept on a formvar-coated copper grid for 30 s and then removed with filter paper. The images were processed using the Gwyddion software.[22] The histograms were computed on a minimum of 100 randomly selected nanoparticles.

The pH of colloidal solution was measured using an Econix 120.

Results and discussion

Gold nanoparticles had a spherical shape (Fig. S1, ESI†) and unimodal size distribution. The average sizes of particles mainly studied were 4.6 ± 0.8 nm and 28.2 ± 3.3 nm.

It was found that in the pH range from 3.5 to 11.5, the optical spectrum of the gold hydrosol exhibits LSPR absorption bands identical in the position and shape with a maximum at 514 ± 1 nm. At pH < 3.5 and pH > 12, the hydrosol loses the aggregate stability, which finally results in precipitation of the metal nanoparticle aggregates (see Fig. S2, ESI†). After injection of hydrogen into the gold hydrosol at pH from 3.6 to 11.5, the LSPR band shifts to shorter wavelengths. Over a period of 15 min, a limiting and stable position of the band is achieved (Fig. 1). The band shape virtually does not change, while the shift of the maximum ($\Delta\lambda_{max}$, nm) increases with an increase in the pH. It was found that $\Delta\lambda_{max}$ increases almost linearly with pH (from 2 ± 0.5 nm at pH 3.6 to 9 ± 0.5 nm at pH 11.1) (Fig. 2).

After evacuation of the hydrosol, the LSPR band returns to the initial position. TEM measurements demonstrated that the injection and subsequent removal of hydrogen have almost no effect on the average size of the gold particles in solution (≈4.6 nm) or on the size distribution. Hence, we can conclude that the reversible shift of the LSPR band is not caused by the aggregation or peptization of nanoparticles.

As will be shown below, the detected shift of the LSPR band of the gold hydrosol is due to dissociative adsorption of

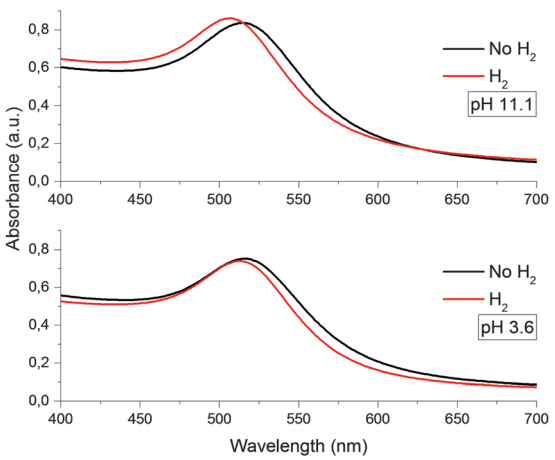

Fig. 1 Optical absorption spectra of gold nanoparticles with an average size of 4.6 nm at various pH.

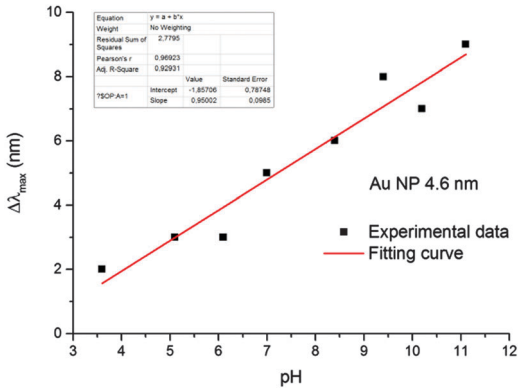

Fig. 2 The pH dependence of the shift of LSPR bands of the gold hydrosol in the solutions saturated by the hydrogen at $[Au_{coll}] = 2 \times 10^{-4}$ mol L^{-1}.

hydrogen, resulting in an increase in the density (concentration) of electrons in the nanoparticles.

In order to confirm the dissociative mechanism of hydrogen interaction with gold nanoparticles in aqueous solution, experiments on Au(III) reduction with gold nanoparticles were performed. In the absence of nanoparticles, Au(III) is not reduced with hydrogen. This is due to the fact that the standard electrode potential of hydrogen $E_0(2H^+/H_2)$ is much higher than the gold potential $E_0(AuCl_4^-/Au^0) = -0.05$ V.[23] Thus, molecular hydrogen cannot reduce Au(III) ions to atoms in bulk solution. Meanwhile, in the presence of nanoparticles, Au(III) ions are efficiently reduced on their surface, as $E_0(AuCl_4^-/Au_{bulk}) = 1.08$ V. That is, the gold nanoparticles catalyze the reduction. Fig. 3a shows the time variation of the absorption spectrum of the hydrosol measured during the reduction of Au(III) ions with hydrogen in a solution with an initial pH of 10.2.

It can be seen that the absorption intensity increases with time. The LSPR band first shifts to longer wavelengths and then gradually narrows down and shifts to shorter wavelengths. After 150 min, the reduction is completed. The observed alteration of the LSPR band is due to the change in the composition of the solution caused by the reaction:

$$2AuCl_4^- + 3H_2 \rightarrow 2Au^0 + 8Cl^- + 6H^+ \quad (1)$$

Consequently, the nanoparticle size increases, the charge state of the surface and the solution composition vary, and, hence, the structure of the electrical double layer at the surface of gold particles changes. Indeed, according to measurements, reduction of a 4×10^{-4} mol L^{-1} solution of Au(III) is accompanied by pH decrease from initial 10.2 to 4.8. In order to prevent the uncontrolled change in the pH, the subsequent investigations of Au(III) reduction were carried out in buffered solutions. As can be seen from Fig. 3b and c, in this case, the increase in the LSPR absorption intensity was no longer accompanied by a shift or change in the shape of the LSPR band. This implies a constant charge state of the particle surface.

Fig. 4–7 show the kinetics of plasmon absorption increase caused by reduction of Au(III) ions with hydrogen in the presence of gold nanoparticles. Since, as noted above, new nanoparticles cannot arise in the system, the increase in the

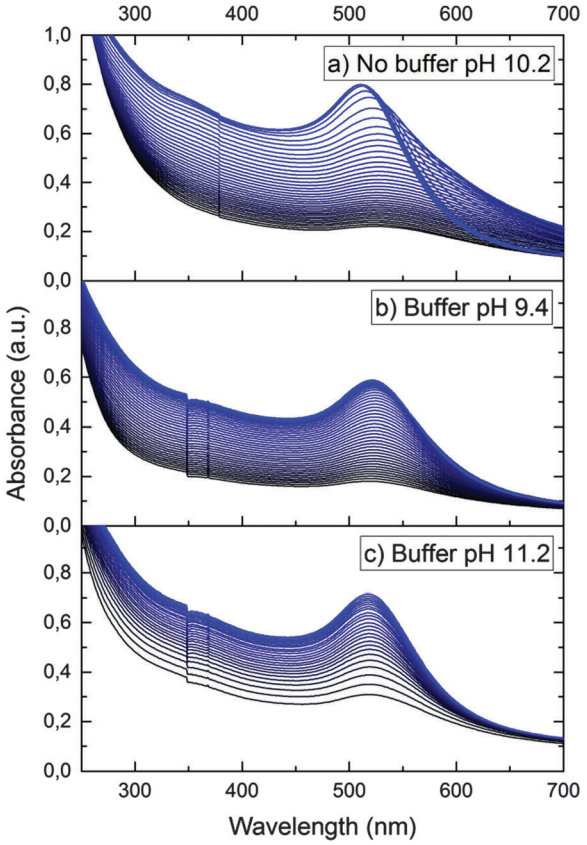

Fig. 3 The change in the absorption spectrum of the gold hydrosol during reduction of Au(III) by hydrogen. The solution $[Au(III)] = 2 \times 10^{-4}$ mol L^{-1}, $[Au_{coll}] = 5 \times 10^{-5}$ mol L^{-1}, $[CitNa_3] = 1.0 \times 10^{-3}$ mol L^{-1}. Time interval between curves is 2 min. The average size of gold nanoparticles is 4.6 nm.

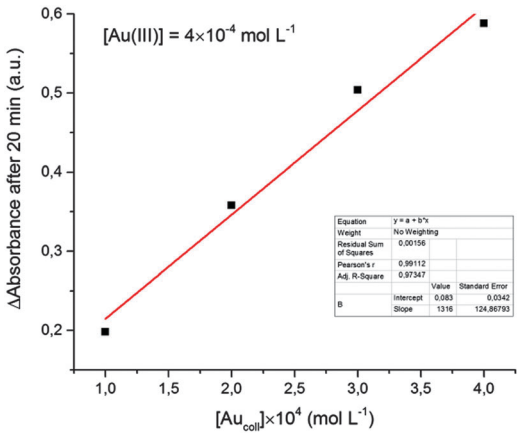

Fig. 4 Absorbance change *vs.* $[Au_{coll}]$ concentration.

absorption can be fully attributed to the growth of the existing particles. This is confirmed by TEM data (Fig. S4, ESI†). As expected, the particle sphericity is simultaneously improved.

Analysis of the kinetics of Au(III) reduction shows a linear proportionality between the reduction rate (determined by the rate of absorption increase in the maximum) and the initial concentration of colloidal gold (Fig. 4). That is, the reaction

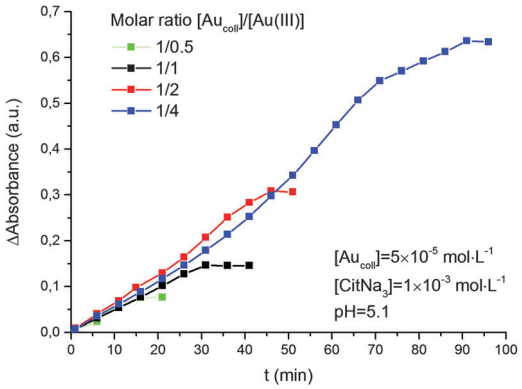

Fig. 5 Kinetics of Au(III) reduction by hydrogen with different molar ratios of $[Au_{coll}]/[Au(III)]$. The average size of gold nanoparticles is 4.6 nm.

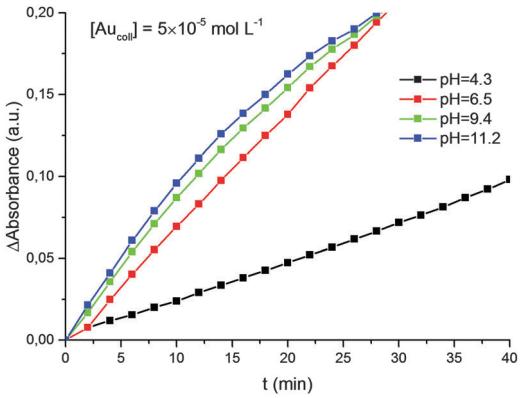

Fig. 6 Kinetics of Au(III) reduction by hydrogen at different pH. The average size of gold nanoparticles is 4.6 nm.

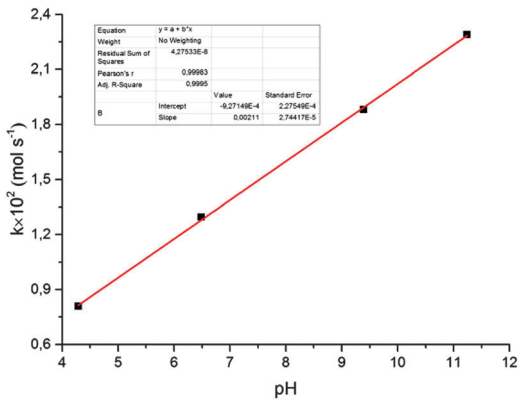

Fig. 7 Rate constant for the reduction of Au(III) ions *vs.* pH.

occurs on the catalyst surface and, as expected, the reaction rate is proportional to the particle surface area. This fact also supports the assumption that the increase in the solution absorbance is due to the increase in the particle size rather than to an increase in the particle concentration. The emergence of new particles would lead to significant deviations from the linear dependence shown in Fig. 4.

It was also shown (Fig. 5) that the rate of reduction does not depend on the concentration of Au(III) ions in solution, *i.e.* the

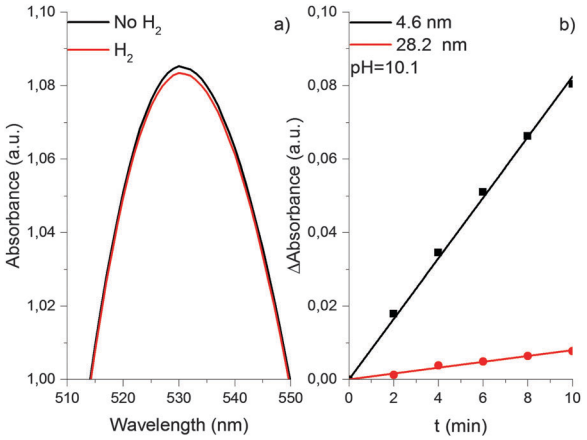

Fig. 8 Optical absorption spectra of gold nanoparticles with an average size of 28.2 nm before and after saturation with hydrogen (a). Kinetics of catalytic reduction of Au(III) on gold nanoparticles with different size (b).

reaction follows a zero-order kinetics. The rate constant for reduction increases with solution pH (Fig. 6). Moreover, there is a strict linear relationship between these parameters (Fig. 7).

The properties of the gold hydrosol described above were studied in detail using 4.6 nm particles. The experiments with other particles demonstrated that an increase in the particle size (from 7.8 to 12.2 nm) is accompanied by a substantial decrease in the shift of the LSPR band caused by saturation of solution with hydrogen. Too small value of $\Delta\lambda_{max}$ shift did not allow us to establish its quantitative correlation with the particle size. Nevertheless, it was reliably established that in the case of particles larger than 20 nm, the saturation of the gold hydrosol with hydrogen does not cause a shift of the LSPR band (see Fig. 8). Particles of such size were also shown to be much less efficient catalysts for the reduction of Au(III) ions with hydrogen. This is demonstrated by Fig. 8b, which presents the initial kinetics of Au(III) reduction in the gold hydrosol with 4.6 nm (black curve) and 28.2 nm (red curve) particles. For 28.2 nm gold particles, the rate of reduction of Au(III) ions is 10.5 ± 1.4 times lower than for 4.6 nm particles. A similar trend was found in the catalytic properties of the gold nanoparticle supported on γ-Al_2O_3. It has been shown that the gold nanoparticles of 3.8, 4.6, and 19.4 nm sizes, unlike the bulk metal, can adsorb hydrogen and catalyze the deuterium–protium exchange in the 77–523 K range. The specific catalytic activity of fine particles (4.6 nm) is 20 times as great as that for coarse particles (19.4 nm).[24] Thus, the catalytic activity substantially decreases with an increase in the gold particle size.

Our investigations indicate that dissociative hydrogen adsorption efficiently takes place on gold nanoparticles with small size. The dissociative adsorption results in accumulation of electrons in nanoparticles. Particles acquire a charge and the higher the pH, the higher the charge. When Au(III) ions are present in the solution, electrons "accrued" by nanoparticles are consumed for reduction of these ions. In other words, nanoparticles act as a sort of "hydrogen-like nanoelectrode" performing electrochemical discharge/ionization reactions. As the nanoparticle size increases, the dissociative adsorption of

hydrogen on gold decreases, and for large particles ($\geq$20 nm), it becomes hardly detectable. Reduced dissociative adsorption is largely responsible for the significant decrease in the Au(III) reduction rate following the increase in the nanoparticle size. Besides, the decrease in the reduction rate is caused by the decrease in the specific surface area of nanoparticles (at fixed gold mass). Calculations show that the ratio of surface atoms in 4.6 and 28.2 nm spherical particles at the same concentration of gold atoms in the hydrosol is equal to approximately 5.5. Experiments show that the Au(III) reduction rate is actually 10.5 $\pm$ 1.4 times higher for 4.6 nm particles. This significant increase in the reduction rate with a decrease in the particle size is, apparently, due to the change in their surface structure. As the particle size decreases, the concentration of structural elements able to atomize the adsorbed hydrogen molecule increases. Indeed, according to published data,[25,26] decreasing gold particle size leads to a decrease in the coordination of gold atoms and an increase in the number of the low-coordination edge and corner sites. A larger number of low-coordination atoms in smaller particles results in enhanced activation and atomization of H_2 molecules on the gold surface. It is generally considered that hydrogen reacts and dissociates on low-coordination gold atoms located at the corners and edges on the surface of gold nanoparticles.[27,28] Ionization of hydrogen atoms is accompanied by accumulation of electrons in the particle, which is manifested as the shift of the LSPR band. This conclusion is supported by the results of ref. 29. It was demonstrated that the active sites for H_2 dissociation are located at the corners and edges on the surface of the gold nanoparticles supported on rutile TiO_2(110). A computational investigation confirmed that the efficiency of dissociative adsorption of H_2 on Au_n clusters increases with decreasing cluster size.

We used the approach developed previously[25,26] to calculate the percentages of edge and corner atoms *versus* the total number of atoms on the nanoparticle surface (see Fig. S3, ESI†). It was found that the proportion of these low-coordination sites, which are likely to catalyze atomization of hydrogen molecules, is approximately 18% for 4.6 nm particles. For 28.2 nm particles, it is only 3%. The decrease in the concentration of the active sites on the gold nanoparticle surface with increasing particle size is apparently responsible for the observed noticeable decrease in the rate of Au(III) reduction with hydrogen.

The nature of particular active sites on the nanoparticle surface and the extent to which they influence the hydrogen atomization and the rate of Au(III) reduction remain obscure. It needs to be kept in mind that the specific surface area and the percentages of edge and corner atoms *versus* the total atoms were calculated with the assumption that the nanoparticles are spherical and have the same size, and the surface corresponds to a perfect crystal structure. In reality, this is not the case. The particle size distribution is fairly broad and the particle shape and crystal structure are not perfect especially for coarse particles. We do not exclude the formation of twinned crystals that can also have an impact on common quantity of edge and corner atoms. It has been also shown that the shape of the gold particles affects the catalytic activity.[30] However, we consider that the small particles observed on TEM images of large particles can exert a stronger impact on kinetics than twinned particles (see Fig. S1, ESI†). Perhaps, it is the reason for catalytic reduction of the Au(III) ions by hydrogen observed for coarse particles.

It is noteworthy that, according to ref. 31, nanogold catalysts exhibit a unique preference toward forming *cis*-2-butene compared to the *trans* isomer, and the ratio of *cis*/*trans* isomers is structure-sensitive in terms of the size of gold nanoparticles. A proportional relationship was revealed: an increase in the fraction of edge + corner atoms following a decrease in the particle size from 9 to 2.7 nm entails a proportional increase in the *cis*-/*trans*-2-butene ratio in the products.

The plasmon absorption of light by gold nanoparticles is a sensitive tool for analysis of the electron state in the metal and redox reactions catalyzed by the nanoparticles. According to the Mie–Drude theory,[32,33] the position of the LSPR peak λ_{max} is inversely proportional to $(n_e)^{1/2}$, where n_e is the concentration of conduction electrons in the metal. The theory predicts a blue shift of the plasmon absorption band with increasing n_e and, conversely, a red shift with decreasing n_e. Correspondingly, upon the adsorption of hydrogen, the LSPR band actually shows a hypsochromic shift, whereas the adsorption of ozone induces, conversely, a bathochromic shift.[14,15] Unfortunately, due to the uncertainty of many parameters used in this theory, it is impossible to calculate the absolute change in the concentration of electrons in gold nanoparticles from the $\Delta\lambda_{max}$ value. However, the positions of bands and the relative concentrations of electrons in the metal core are related by the simple expression

$$\frac{n_e^f}{n_e^i} = \left(\frac{\lambda_{max}^i}{\lambda_{max}^f}\right)^2, \quad (2)$$

where superscripts i and f refer to (conventionally) the initial and final states of the nanoparticle in some process with the change in the concentration of electrons. Hence, the variation of the relative concentration of electrons in the metal can be estimated from the shift of the LSPR band. Thus, for the observed shift of the LSPR band of the gold hydrosol (4.6 nm particles), which is 10 nm at pH 11 and approximately 2 nm at pH 3.6, the relative concentration of electrons in the metal increases by 4% and 0.7%, respectively.

Eqn (2) can be rearranged as follows. Considering that $n_e^f = n_e^i + \Delta n_e$ and $\lambda_{max}^i = \lambda_{max}^f + \Delta\lambda$ and neglecting the higher powers of small value $\Delta\lambda/\lambda_{max}^f$ ($\leq$6%), one gets

$$\Delta n_e \approx \frac{2n_e^i}{\lambda_{max}^f}\Delta\lambda \quad (3)$$

This equation explicitly establishes a direct correlation between the change in the concentration of electrons in a metal nanoparticle and the shift of the LSPR band. The greater the shift of the band, the higher the change in the concentration of electrons.

It is evident that the change in the potential is proportional to the change in the concentration of excess electrons in the particle,

$$\Delta\varphi_p = -ke\Delta n_e \quad (4)$$

The minus sign indicates that the addition of electrons to a particle decreases its potential, so that the constant k is positive. Comparison of eqn (3) and (4) shows that the greater the shift of the LSPR band, the lower the nanoparticle potential.

Formula (4) can be substantiated as follows. We will use the known formula describing the potential variation near a charged spherical particle of radius R placed into a bipolar environment (electrolyte, plasma)[34]

$$\varphi(r) = \frac{q}{\varepsilon r(1+kR)}\exp[-k(r-R)] \quad (5)$$

where q is the particle charge (in our case, $q = -e\Delta n_e V_p$), $V_p = 4/3\pi R^3$ is the particle volume, ε is the dielectric permittivity of the electrolyte, k is the inverse Debye length, and r is the distance from the particle centre. The Debye length is known to depend on the electrolyte concentration c (mol L^{-1}) as $k^{-1} = 3 \times 10^{-8}c^{-1/2}$ cm ($0.304c^{-1/2}$ nm).[35] In our case, the electrolyte concentration is about 10^{-4} mol L^{-1}. Therefore, the Debye length is almost an order of magnitude greater than the nanoparticle radius ($kR \ll 1$). Thus, its potential (actually $\Delta\varphi_p$) can be expressed using the simple relation

$$\Delta\varphi_p = -\frac{e\Delta n_e V_p}{\varepsilon R} = -ke\Delta n_e \quad (6)$$

The parameter k introduced above can be easily found from eqn (5).

Thus, we assume that hydrogen molecules are dissociatively adsorbed on gold nanoparticles that lead to accumulation of electrons in the metal. Hydrogen is ionized on colloid gold particles as on nanoelectrodes, according to the equation

$$H_2 + Au_{coll}(n_e) \rightleftarrows 2H^+ + 2e \quad (7)$$

As electrons are accumulated on a colloid particle, the particle potential decreases, and after some time, hydrogen ionization reaction slows down. As a result, electrochemical equilibrium is established with some limiting potential of particles which is characteristic of the given conditions (first of all, pH). The time required to reach the equilibrium potential can be estimated experimentally as the time necessary for the LSPR band to reach a stationary position. As shown by experiments, the time required is approximately 15 minutes. When hydrogen is removed, equilibrium (7) shifts, correspondingly, to the left. The LSPR band shifts to longer wavelengths.

The equilibrium constant for reaction (7) is given by

$$K(T) = \frac{[n_e]^2[H^+]^2}{[Au_{coll}][H_2]} = \exp\left(-\frac{G}{kT}\right) \quad (8)$$

where ΔG is the change in the Gibbs energy for the reaction, n_e is the concentration of free electrons in the particles.

Furthermore, electron transfer towards a nanoparticle (or back) can occur repeatedly. Therefore, an increase and/or decrease in the concentration of electrons in the particle (unlike the bulk electrode) leads to a change in ΔG and the particle potential. Therefore, we will write ΔG in the form

$$\Delta G = \Delta G^* - e\Delta\varphi_p, \quad (9)$$

where $\Delta\varphi_p$ is the change in the particle potential induced by electron transfer, e is the proton charge (the minus sign in eqn (9) implies that a decrease in the particle potential should retard the electron transfer toward the particle), and ΔG^* takes account of all the possible contributions to the reactions.

Having employed the above equations, one has

$$\exp\left(-\frac{(\Delta G^* - ke\Delta n_e)}{RT}\right) = \frac{[n_e]^2[H^+]^2}{[Au_{coll}][H_2]} \quad (10)$$

The concentration of colloid gold particles does not change during the redox process and the hydrogen concentration also remains almost invariable. The change in the number of electrons caused by hydrogen ionization is small compared with the total number of free electrons in the particles. Thus, in the right hand side of eqn (10), $n_e = n_{e0} + \Delta n_e$ and $\Delta n_e \ll n_{e0}$. This inequality allows using in the right hand side of eqn (10) n_{e0} instead of n_e, when finding dependence on pH. The use of n_e contributes little to the final result. These considerations lead us to the following expression after taking the logarithm of eqn (9):

$$\Delta n_e = A^* - B^* \ln[H^+] = A + B\ \mathrm{pH}, \quad (11)$$

where B is the positive constant. One can see than the concentration of electrons in nanoparticles linearly increases with pH.

In view of the relationship between Δn_e and $\Delta\lambda$ (eqn (3)), one gets

$$\Delta\lambda \approx \frac{\lambda^f_{max}}{2n^i_e}(A + B\mathrm{pH}) \quad (12)$$

Thus, the shift of the LSPR band of the gold hydrosol should be a linear function of pH. As can be seen, this is in line with the experimental data (see Fig. 2). It also follows from eqn (4) and (11) that the particle potential also linearly increases with pH.

$$\Delta\varphi_p = -ke(A + B\ \mathrm{pH}) \quad (13)$$

In other words, the change in the electrochemical potential follows a linear dependence on the pH value inherent in a conventional hydrogen electrode and expressed by the known equation $E = E^0 - 0.059$ pH but with its own coefficient.

Now we will consider the reduction of Au(III) ions with hydrogen on gold nanoparticles. This process can be treated, with a sufficient reason, as an electrode reaction, because it is based on the step of transfer of charged species (electrons) through an interface typical of electrochemical processes. Moreover, discharge/ionization is the rate-limiting step in the complex electrode process. It can be described by the following reaction scheme. As a result of dissociative adsorption of hydrogen, electrons are accumulated on the gold particle (particle charging). When a sufficient number of electrons has been accumulated on the nanoparticle, the potential of

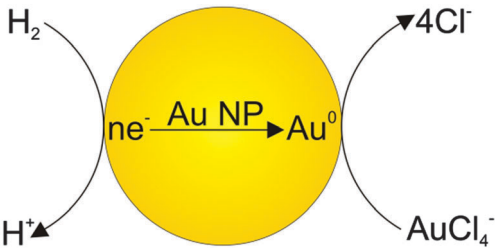

Fig. 9 Scheme of the electrochemical process on the gold nanoelectrode.

the particle reaches a value at which reduction of Au(III) ions takes place. The electrochemical process on the gold nanoelectrode is vividly depicted in Fig. 9.

During this reaction, the excess of electrons decreases (particle discharge). This results in a decrease in the particle potential. Hence, the Au(III) reduction slows down. Finally, a dynamic equilibrium is established in which the particle charging and discharge rates are equal. This gives rise to a quasi-steady state in which the particle potential is somewhat smaller (in magnitude) than that specified by formula (13) and which corresponds to thermodynamic equilibrium in the absence of Au(III) reduction. The potential of the quasi-steady state is determined by the ratio of rate constants for particle charging and discharge.

As noted above, the rate of reaction does not depend on the Au(III) concentration and linearly increases with an increase in the pH. The former fact indicates that particle charging, *i.e.*, dissociative adsorption and the related electron transfer, is the rate-limiting step in the Au(III) reduction. The linear dependence of the rate on the pH can be established from consideration of electrochemical processes with the assumption that the properties of gold particles (electrodes) do not change significantly during the process.

On conventional electrodes, electrochemical reduction of metal ions proceeds if some overpotential (in magnitude) is present on the electrode. According to the Faraday law, the rate of electrolytic deposition of the metal V does not depend on the concentration of cations in solution and is determined by the current intensity:

$$V(M) = \mu I, \tag{14}$$

Here I is the current intensity, μ is the electrochemical equivalent, and M stands for metal.

The same pattern is quite applicable to nanoparticles. Note only that the overpotential on gold nanoparticles appears in our case as a result of reaction (7) and is caused by excess concentration of electrons determined by relation (11). As has already been noted, the rate-limiting step is the accumulation of excess electrons upon hydrogen adsorption and dissociation, whereas Au(III) reduction is comparatively fast. This means that the steady-state potential established on the particles is close to E_0 (for nanoparticles, this value can certainly differ from that found for the bulk electrode but we will designate it by the same symbol). Since the overpotential and the concentration of electrons are interrelated, some stationary concentration of excess electrons on nanoparticles is obviously also established, so that the rate of removal of the excess electrons *via* reaction (1) is equal to the rate of their arrival by reaction (7):

$$\frac{dn_e^-}{dt} = \frac{dn_e^+}{dt} \tag{15}$$

According to (14), the current generated upon hydrogen ionization on the gold nanoelectrode is given by $I = Ldn_e^-/dt$, where L is the geometric factor. Then gold electrodeposition *via* reduction of Au(III) with hydrogen can be described as

$$V(Au^0) = \mu L \frac{dn_e^+}{dt} \tag{16}$$

According to the general principles of thermodynamics of irreversible processes,[36] the generalized thermodynamic flux (in our case, just electric current) is proportional to the deviation of the appropriate thermodynamic quantity (thermodynamic force) from equilibrium. Basing on these principles, one can assume that the rate of arrival of excess electrons (thermodynamic flux) will be proportional to the difference between the potential $\Delta\varphi_p$ equilibrium for reaction (7) and the instantaneous potential of the particles (thermodynamic force). It follows from the foregoing that the instantaneous potential can be identified with E_0; hence, one gets

$$\frac{dn_e^+}{dt} = \Lambda\left(\Delta\varphi_p - E_0\right) \tag{17}$$

where Λ is a phenomenological kinetics coefficient.

Then, taking account of relations (14)–(17) gives

$$V(Au^0) = \mu L\Lambda(\Delta\varphi_p - E^0) = A_{ef} + B_{ef}\,pH \tag{18}$$

Here we used formula (13) and introduced new coefficients A_{ef} and B_{ef}, the relation of which to preceding parameters is very simply established. Note that the possible pH dependence of the potential E_0 for a nanoparticle (it can be reasonably expected to be virtually the same as for bulk electrodes) will have no effect on the right-hand part of eqn (18). It will affect only A_{ef} and B_{ef} values. Thus, the presented considerations indicate that the Au(III) reduction rate should linearly depend on pH, that is observed in the experiment. Note also that the rate is proportional to the nanoparticle concentration in solution, *i.e.*, as expected, it is proportional to the overall surface area of the electrode.

Conclusions

The presented results indicate that dissociative adsorption of hydrogen molecules accompanied by accumulation of electrons in the metal takes place on gold nanoparticles in colloid solution. That is, the situation is similar to electrochemical reactions on a hydrogen electrode. The processes are reflected and recorded in the variation of the LSPR. This fact provides very important information on the mechanisms of reactions catalyzed by gold nanoparticles. In particular, accumulation of electrons in the particles induces an increase (in magnitude) of

the overpotential of particles and a shift of the plasmon resonance band to shorter wavelengths. The dependence of the overpotential on the pH typical of a hydrogen electrode is manifested. If Au(III) ions are present in the solution, they are deposited on gold particles. The reduction rate does not depend on the concentration of gold ions. The rate-limiting step of the reaction is dissociative adsorption of hydrogen molecules. The reduction rate is determined by the overpotential and depends linearly on the pH. With increasing size of gold nanoparticles, their ability to accumulate excess electrons by the dissociative mechanism decreases and the Au(III) reduction rate becomes lower. High sensitivity of optical absorption of gold nanoparticles to electron donors and acceptors and to the composition of the environment allows effective use of LSPR spectroscopy to study the mechanism of catalytic reactions.

Acknowledgements

This work was supported by the Russian Foundation for Basic Research, project no. 15-03-02068-a.

Notes and references

1 M. Haruta, *Catal. Today*, 1997, **36**, 153–166.
2 G. C. Bond and D. T. Thompson, *Catal. Rev.: Sci. Eng.*, 1999, **41**, 319–388.
3 O. Lopez-Acevedo, K. A. Kacprzak, J. Akola and H. Häkkinen, *Nat. Chem.*, 2010, **2**, 329–334.
4 Y.-S. Bao, M. Baiyin, B. Agula, M. Jia and B. Zhaorigetu, *J. Org. Chem.*, 2014, **79**, 6715–6719.
5 S. K. Ghosh and T. Pal, *Chem. Rev.*, 2007, **107**, 4797–4862.
6 A. Henglein, P. Molvaney and T. Linnert, *Faraday Discuss.*, 1991, **92**, 31–44.
7 A. Henglein and D. Meisel, *Langmuir*, 1998, **14**, 7392–7396.
8 B. G. Ershov and A. V. Gordeev, *Mendeleev Commun.*, 2001, **4**, 147–148.
9 T. Ung, M. Giersig, D. Dunstan and P. Mulvaney, *Langmuir*, 1997, **13**, 1773–1782.
10 P. Mulvaney, J. Pérez-Juste, M. Giersig, L. M. Liz-Marzán and C. Pecharromán, *Plasmonics*, 2006, **1**, 61–66.
11 P. A. Morozov, B. G. Ershov, E. V. Abkhalimov, O. V. Dement'eva, T. B. Rumyantseva, V. M. Rudoy and V. I. Roldughin, *Colloid J.*, 2011, **73**, 668–675.
12 P. A. Morozov, B. G. Ershov, E. V. Abkhalimov, O. V. Dement'eva, M. A. Filippenko, V. M. Rudoy and V. I. Roldughin, *Colloid J.*, 2012, **74**, 502–509.
13 B. G. Ershov, E. V. Abkhalimov, V. I. Roldughin, V. M. Rudoy, O. V. Dement'eva and R. D. Solovov, *Phys. Chem. Chem. Phys.*, 2015, **17**, 18431–18436.
14 S. D. Puckett, J. A. Heuser, J. D. Keith, W. U. Spendel and G. E. Pacey, *Talanta*, 2005, **66**, 1242–1246.
15 A. N. Pisarenko, W. U. Spendel, R. T. Taylor, J. D. Brown, J. A. Cox and G. E. Pacey, *Talanta*, 2009, **80**, 777–780.
16 B. G. Ershov, V. I. Roldughin, E. V. Abkhalimov, R. D. Solovov, O. V. Dement'eva and V. M. Rudoy, *Colloid J.*, 2014, **76**, 308–313.
17 R. D. Solovov and B. G. Ershov, *Colloid J.*, 2014, **76**, 595–599.
18 C. J. Johnson, E. Dujardin, S. A. Davis, C. J. Murphy and S. Mann, *J. Mater. Chem.*, 2002, **12**, 1765–1770.
19 J. Turkevich, P. C. Stevenson and J. Hillier, *Discuss. Faraday Soc.*, 1951, **11**, 55–75.
20 B. V. Enutsun and J. Turkevich, *J. Am. Chem. Soc.*, 1963, **85**, 3317–3328.
21 H. T. S. Britton and R. A. Robinson, *J. Chem. Soc.*, 1931, 1456–1462.
22 D. Necas and P. Klapetek, *Cent. Eur. J. Phys.*, 2012, **10**, 181–188.
23 B. G. Ershov, *Russ. Chem. Rev.*, 1981, **50**, 1119–1133.
24 O. A. Boeva, B. G. Ershov, K. N. Zhavoronkova, A. A. Odintsov, R. D. Solovov, E. V. Abkhalimov and N. D. Evdokimenko, *Dokl. Phys. Chem.*, 2015, **463**, 165–167.
25 S. Schimpf, M. Lucas, C. Mohr, U. Rodemerck, A. Bruckner, J. Radnik, H. Hofmeister and P. Claus, *Catal. Today*, 2002, **72**, 63–78.
26 R. Van Hardeveld and F. Hartog, *Surf. Sci.*, 1969, **15**, 189–230.
27 C. Mohr, H. Hofmeister, J. Radnik and P. Claus, *J. Am. Chem. Soc.*, 2003, **125**, 1905–1911.
28 E. Bus, J. T. Miller and J. A. van Bokhoven, *J. Phys. Chem. B*, 2005, **109**, 14581–14587.
29 A. Lyalin and T. Taketsugu, *Faraday Discuss.*, 2011, **152**, 185–201.
30 C. Mohr, H. Hofmeister and P. Claus, *J. Catal.*, 2003, **213**, 86–94.
31 X.-F. Yang, A.-Q. Wang, Y.-L. Wang, T. Zhang and J. Li, *J. Phys. Chem. C*, 2010, **114**, 3131–3139.
32 C. F. Bohren and D. R. Huffman, *Absorption and Scattering of Light by Small Particles*, Willey, New York, 1983.
33 U. Kreibig and M. Vollmer, *Optical Properties of Metal Clusters*, Springer, Berlin, 1995.
34 R. Kubo, *Statistical Mechanics*, Amsterdam, North-Holland, 1965.
35 D. H. Everett, *Basic Principles of Colloid Science*, The R. Soc. Chem., London, 1988.
36 S. R. de Groot and P. Mazur, *Non-Equilibrium Thermodynamics*, Amsterdam, North-Holland, 1962.